JSHC
Japan Society of
Histochemistry and Cytochemistry
Established 1959

Acta Histochem. Cytochem. 48 (5): 135–143, 2015
doi: 10.1267/ahc.15010

Increased Expression of Osteopontin in the Degenerating Striatum of Rats Treated with Mitochondrial Toxin 3-Nitropropionic Acid: A Light and Electron Microscopy Study

Hong-Lim Kim[1,4], Mun-Yong Lee[3], Yoo-Jin Shin[3], Doo-Won Song[2], Jieun Park[4], Byung-Soo Chang[5] and Jong-Hwan Lee[1]

[1]Department of Veterinary Anatomy, College of Veterinary Medicine, Konkuk University, Seoul 143–701, Korea, [2]Department of Veterinary Internal Medicine, College of Veterinary Medicine, Konkuk University, Seoul 143–701, Korea, [3]Department of Anatomy, College of Medicine, Catholic University, Seoul 137–701, Korea, [4]Integrative Research Support Center, College of Medicine, Catholic University, 137–701, Seoul, Korea and [5]Department of Cosmetology, Hanseo University, 356–706, Seosan, Chungnam, Korea

Received May 19, 2015; accepted September 4, 2015; published online October 21, 2015

The mycotoxin 3-nitropropionic acid (3NP) is an irreversible inhibitor that induces neuronal damage by inhibiting mitochondrial complex II. Neurodegeneration induced by 3NP, which is preferentially induced in the striatum, is caused by an excess influx and accumulation of calcium in mitochondria. Osteopontin (OPN) is a glycosylated phosphoprotein and plays a role in the regulation of calcium precipitation in the injured brain. The present study was designed to examine whether induction of OPN protein is implicated in the pathogenesis of 3NP-induced striatal neurodegeneration. We observed overlapping regional expression of OPN, the neurodegeneration marker Fluoro-Jade B, and the microglial marker ionized calcium-binding adaptor molecule 1 (Iba1) in the 3NP-lesioned striatum. OPN expression was closely associated with the mitochondrial marker NADH dehydrogenase (ubiquinone) flavoprotein 2 in the damaged striatum. In addition, immunoelectron microscopy demonstrated that OPN protein was specifically localized to the inner membrane and matrix of the mitochondria in degenerating striatal neurons, and cell fragments containing OPN-labeled mitochondria were also present within activated brain macrophages. Thus, our study revealed that OPN expression is associated with mitochondrial dysfunction produced by 3NP-induced alteration of mitochondrial calcium homeostasis, suggesting that OPN is involved in the pathogenesis of striatal degeneration by 3NP administration.

Key words: osteopontin, 3-nitropropionic acid, mitochondria, microglia

I. Introduction

Mitochondrial disturbances, such as inhibition of the mitochondrial respiratory chain and excessive oxidative stress, are involved in many neurological disorders [23]. In animal models of brain ischemia, an overload of intracellular calcium leads to impairments in mitochondrial respiration, followed by cell death [5, 15, 21, 35, 39, 46, 52]. Ultrastructural observations after administration of excitotoxic drugs such as kainic or ibotenic acid show the presence of calcium precipitates in the mitochondria of damaged neurons [16, 34, 48].

3-Nitropropionic acid (3NP) is a natural mycotoxin characteristic to fungi infecting leguminous plants which causes disease in cattle and man [9, 28]. It is used to generate disease models of striatal neurodegeneration, particularly Huntington's disease (HD), with which it shares

Correspondence to: Jong-Hwan Lee, DVM Ph.D, Department of Veterinary Anatomy, College of Veterinary Medicine, Konkuk University, 120 Neungdong-Ro, Gwangin-Gu, Seoul, 143–701, Korea.
E-mail: jhlee21@konkuk.ac.kr

similar anatomical, histopathological, and neurochemical changes [4, 7, 9, 24, 36]. When 3NP is directed into the striatum of rodents, a specific lesion accompanied by striatal neuronal loss and astroglial proliferation is produced. This lesion closely resembles the above-mentioned pathological features of HD [4, 8, 9, 22, 49, 53]. 3NP is an irreversible inhibitor of mitochondrial complex II (i.e., succinate dehydrogenase), and thus directly impairs mitochondrial oxidative metabolism and causes subsequent neuronal cell death [2, 4, 11]. Neurodegeneration induced by 3NP involves changes in mitochondrial permeability transition (MPT). These changes are caused by the accumulation of excessive calcium in the mitochondria, which results in swelling of the organelles, a decrease in transmembrane potential, loss of ATP synthesis, and release of pro-apoptotic factors such as cytochrome c [3, 20, 26, 29, 30, 42, 54].

Osteopontin (OPN) is a secreted glycosylated phosphoprotein with an arginine-glycine-aspartate (RGD) motif that binds to multiple integrin subunits and CD44 variants [51]. This phosphoprotein is involved in numerous pathophysiological processes, including regulation of inflammation, wound repair, cell-mediated immunity, and metastatic spread of various cancers [14, 40]. Its expression has been widely studied in various pathological conditions including cancer and both ischemic and toxicant injuries in many tissues and organs. In addition, recent evidence observed that OPN is closely associated with calcium precipitation. By binding to calcium deposits, OPN is involved in the mechanisms by which such deposits are scavenged in the ischemic brain [44]. Thus, we hypothesize that following 3NP administration, OPN would be associated with calcium precipitation within mitochondria that could lead to selective degeneration of the caudate-putamen [19]. However, to the best of our knowledge, there are no data on the *in vivo* expression of OPN in 3NP models. Since the selective impairment produced by 3NP may contribute to the understanding of OPN function in the central nervous system, we assessed the cellular localization of OPN in the striatum after 3NP injury via confocal and immunoelectron microscopy.

II. Materials and Methods

Animals

All experimental procedures were conducted according to the guidelines of the Institutional Animal Care and Use Committee at Konkuk University, Seoul, Korea. Female Sprague-Dawley rats (n=10) weighing 300–320 g were used in this study. 3-nitropropionic acid (3NP; Sigma-Aldrich, St. Louis, MO, USA) was dissolved in saline solution, and the pH was adjusted to 7.4 with NaOH. Animals received a subcutaneous injection of 3NP (15 mg/kg) for 4 weeks, once every two days. Animals were anesthetized with chloral hydrate (400 mg/kg, intraperitoneally) and sacrificed 2 days after the final injection. Control rats received the equivalent volume of normal saline solution. To evaluate tissue injury by 3NP, brains (n=3) were quickly removed and were sliced at 1-mm thickness. Brain slices were incubated at 37°C for 30 min in a 2% solution of 2,3,5-triphenyltetrazolium chloride (TTC; Sigma-Aldrich).

Double immunohistochemistry

Brain samples were cryoprotected and frozen in liquid nitrogen. For immunofluorescence, semithin cryosections (1 μm thick) were cut at −80°C on a Leica EM UC7 ultramicrotome equipped with an FC7 cryochamber. For double labeling studies, brain sections were first incubated in a blocking buffer (1% bovine serum albumin; BSA) in phosphate buffered-saline (PBS) in a dark humidified chamber for 1 hr at room temperature, and then incubated at 4°C overnight with a mixture of mouse monoclonal anti-OPN (American Research Products, Belmont, MA; dilution 1:150), plus one of either rabbit polyclonal antibodies to ionized calcium-binding adaptor molecule 1 (Iba1; Wako Pure Chemical Industries, Japan; dilution 1:500), or NADH dehydrogenase (ubiquinone) flavoprotein 2 (NDUFV2; Proteintech, USA; dilution 1:100). Sections were then washed 3 times in PBS (5 min each), and incubated for 2 hr at room temperature with the following secondary antibodies: Cy3-conjugated donkey anti-mouse (Jackson ImmunoResearch, West Grove, PA, USA; dilution 1:2000) and Alexa Fluor 488 goat anti-rabbit (Molecular Probes, Eugene, OR, USA; 1:300) for OPN/Iba1 double labeling, and Cy3-conjugated donkey anti-rabbit and Alexa Fluor 488 goat anti-mouse for OPN/NDUFV2 double labeling. Counterstaining of cell nuclei was carried out using 4',6-diamidino-2-phenyindole (DAPI; Roche, Germany; dilution 1:1000) for 10 min. Slides were viewed and photographed using a confocal microscope (LSM 510 Meta; Carl Zeiss Co. Ltd., Germany). Images were converted to TIFF format, and contrast levels were adjusted using Adobe Photoshop v7.0.

Fluoro-Jade B staining and osteopontin immunohistochemistry

To simultaneously detect OPN protein and degenerating cells, we used immunohistochemistry for OPN and Fluoro-Jade B (FJB; Millipore, Temecula, CA, USA) histochemistry. After immunostaining for OPN, sections were transferred to a solution of 0.06% potassium permanganate for 10 min and then to a solution of 0.0004% FJB for 30 min. Sections were washed 3 times in distilled water, fully dried, cleared in xylene, and examined under a confocal laser scanning microscope.

Immunoelectron microscopy

For electron microscopy, pre-embedding immunoperoxidase and immunogold/silver staining methods were used. For immunoperoxidase staining, 50 μm thick vibratome sections were incubated in 1% BSA in 0.01 M PBS, and then incubated with mouse monoclonal anti-rat OPN

antibody at 4°C overnight. Sections were washed 3 times (5 min each) with PBS, incubated for 2 hr with biotinylated goat anti-mouse IgG in 0.01 M PBS at room temperature, and then washed 3 times (5 min each) with PBS. The immunoreaction was visualized using diaminobenzidine as the chromogen. After postfixation in 1% glutaraldehyde and 1% osmium tetroxide in phosphate buffer for 30 min each, dehydration in a graded series of ethanols, and flat embedding in Epon 812 resin, the areas of interest were excised and glued onto resin blocks. Ultrathin sections (70 to 90 nm thick) were cut on an ultramicrotome, stained with 1% uranyl acetate, and observed in an electron microscope (JEM 1010, JEOL, Tokyo, Japan). For immunogold-silver labeling, vibratome sections were incubated with the primary antibodies as above. Sections were then incubated with an anti-mouse secondary antibody conjugated to nanogold particles (1 nm) (Nanoprobes, Stony Brook, NY; dilution 1:100) for 2 hr. Silver enhancement was performed using the HQ silver enhancement kit (Nanoprobes) for 3 min. Ultrathin sections were prepared as described above, and observed using an electron microscope.

Co-localization analyses

To measure co-localization between OPN and NDUFV2, three regions of interest in the 3NP-injured core, from five sections per animal (n=5), were randomly captured at ×400 magnification using the confocal microscope. A statistical measure of the fluorescent ratio of colocalization was conducted using ZEN2009 software (Carl Zeiss Co. Ltd., Germany).

III. Results

Localization of osteopontin in the damaged striatum after 3NP-induced neurotoxicity

TTC staining revealed clear, bilateral striatal lesions including the majority of the striatum, whereas no striatal lesions were observed in control rats that received saline instead of 3NP (Fig. 1). To verify whether 3NP-induced neuronal damage in the striatum was closely associated with OPN, we examined OPN immunoreactivity and FJB staining, a fluorescent marker for neurodegeneration. Double-labeling studies showed overlapping regional distribution of OPN and FJB staining in the striatum of 3NP-treated rats. Both labels were confined to the lesion core, resulting in a clear demarcation of the lesion core and the lesion rim (Fig. 2A–C). At higher magnification, OPN immunoreactivity in the lesion core appears in the FJB-labeled cells, which were identified as degenerating neurons lacking nuclear staining with DAPI (Fig. 2D–F). By contrast, no significant immunoreactivity for OPN was detected in the striatum of control rats (see Fig. 4A, B).

We also examined whether OPN labeling was present in Iba1-positive microglia, which have been previously reported to express OPN [43, 44]. As shown in Fig. 2D–F, overlapping regional expression of OPN and Iba1 immunoreactivity was also observed in the core of the 3NP-lesioned striatum, where both antigens were highly expressed.

Fig. 1. Representative brain slice stained by 2,3,5-triphenyltetrazolium chloride (TTC) in control rats that received saline (**A**) and 3-nitropropionic acid (3NP)-injured rats (**B**). TTC staining revealed the manifest bilateral striatal lesions including the majority of the striatum, whereas no striatal lesions were observed in control rats that received saline.

Parallel distribution of osteopontin and NDUFV2 immunofluorescence in the damaged striatum after 3NP-induced neurotoxicity

To identify the spatial relationship of OPN expression in the mitochondria at the core of the lesion, we conducted a double immunofluorescence labeling study. As shown in Fig. 3A–D, most of the punctate OPN immunoreactivity was colocalized with the mitochondrial marker NDUFV2 (76.2% on average). However, some relatively large OPN clusters did not show NDUFV2 immunolabeling.

Ultrastructural localization of osteopontin in the damaged striatum after 3NP-induced neurotoxicity

We conducted and immunoelectron microscopy survey to study the subcellular distribution of OPN in degenerated neurons in 3NP-lesioned rats. OPN protein was not expressed in normal rat striatum (Fig. 4A), and normal striatal mitochondria clearly showed cristae and the archetypal regular, round shape (Fig. 4B). OPN-immunoreactive profiles, as revealed by electron-dense precipitate, were observed scattered in degenerating neurons located throughout the lesion core (Fig. 4C). At higher magnification, the profiles could be identified as mitochondria with recognizable internal cristae (Fig. 4D). In addition, cell fragments containing OPN-labeled mitochondria were phagocytized by activated microglia (Fig. 4E–H).

Silver-enhanced immunogold labeling allowed further analysis of ultrastructural characteristics of OPN-labeled mitochondria. Silver-enhanced gold particles used for the detection of OPN were primarily localized to the inner membrane and matrix of mitochondria in degenerating neuritic profiles (Fig. 5A, B). There seemed to be a noticeable

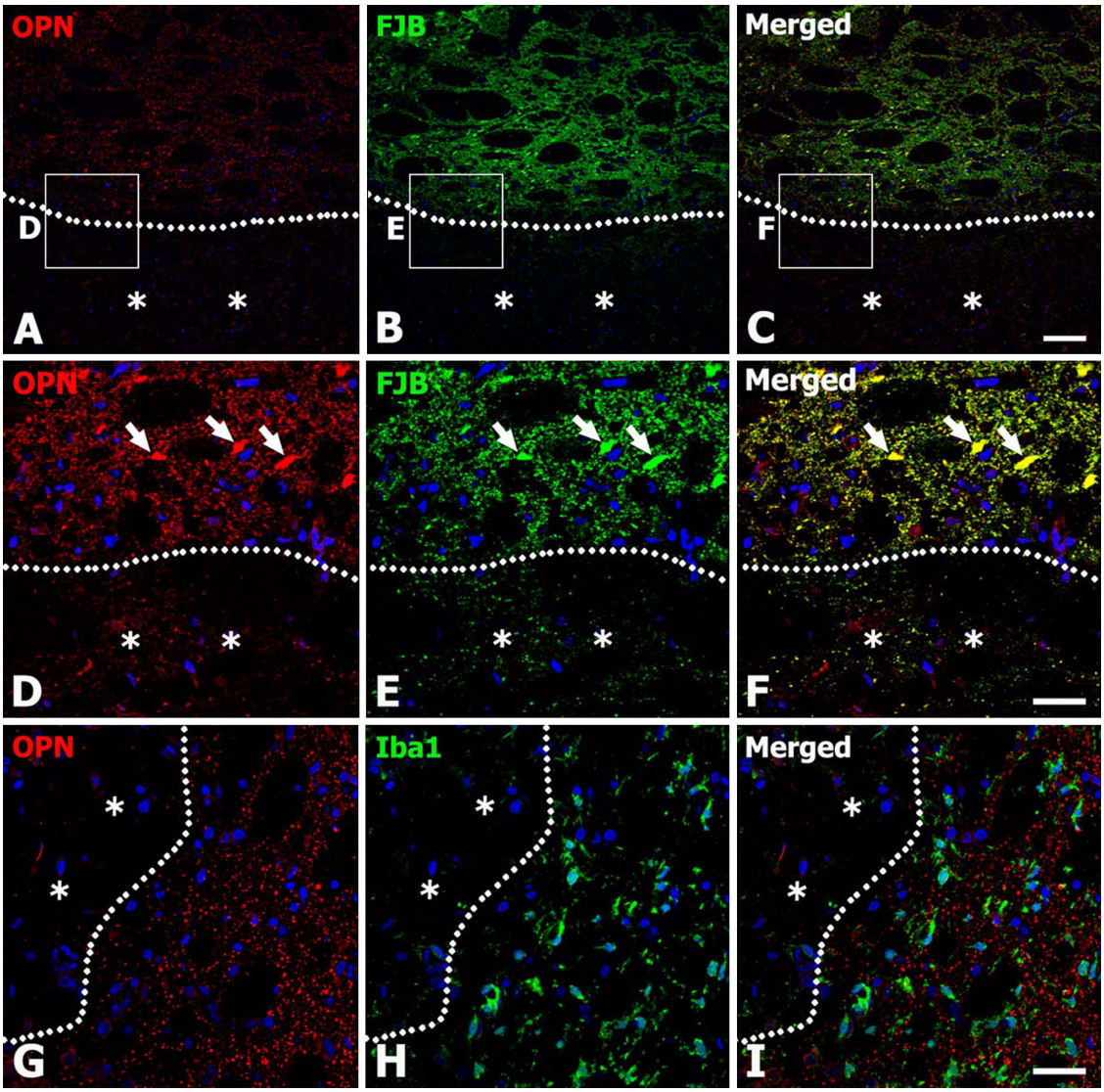

Fig. 2. Relation between osteopontin (OPN) expression and 3-nitropropionic acid (3NP)-injured striatum demonstrated using confocal microscopy. (**A–C**) Double labeling for OPN and Fluoro-Jade B (FJB) staining showing that OPN and FJB staining is restricted to the lesion core. The broken line indicates the border between the lesion core and the rim of the lesion (asterisks). (**D–F**) Higher magnification views of the boxed area in **A–C**. These images show OPN (**D**) and FJB (**E**) immunoreactivity, as well as a merged image of both immunolabels (**F**) and degenerating neurons (arrow in **D–F**). (**G–I**) Double labeling for OPN and Iba1 in the 3NP-lesioned striatum. A number of Iba1-positive microglial cells appear in areas that present OPN immunolabeling. The broken line indicates the border between the lesion core and the rim of the lesion (asterisks). Bars=100 μm (**A–C**); 30 μm (**D–I**).

increase in the number of gold particles present in swollen mitochondria compared to normal-appearing mitochondria, suggesting that OPN protein was preferentially localized to damaged mitochondria. The accumulation of immunogold particles was usually observed inside mitochondria (Fig. 5C, E), while gold particles were occasionally localized along the surface of, but not within mitochondria, in cases where the mitochondria themselves appeared to be small and relatively electron-dense (Fig. 5D).

IV. Discussion

The present study demonstrates for the first time that OPN protein was localized to the mitochondria of degenerating neurons in the core of the 3NP-induced lesion. OPN expression was induced in the lesion core after systemic administration of 3NP, while at the same time we replicated previous findings demonstrating that the undisturbed striatum does not express OPN [43, 44]. Double immunolabeling showed that OPN was closely associated with the NDUFV2 mitochondrial marker in the 3NP-lesioned striatum. Furthermore, using immunogold-silver electron microscopy we confirmed that OPN was localized to the inner membrane and matrix of the swollen mitochondria found in degenerating neurons in the lesion core. It is interesting that when the mitochondria appeared to be small and highly condensed, OPN protein was occasionally localized along the surface of, but not within the mitochondria (com-

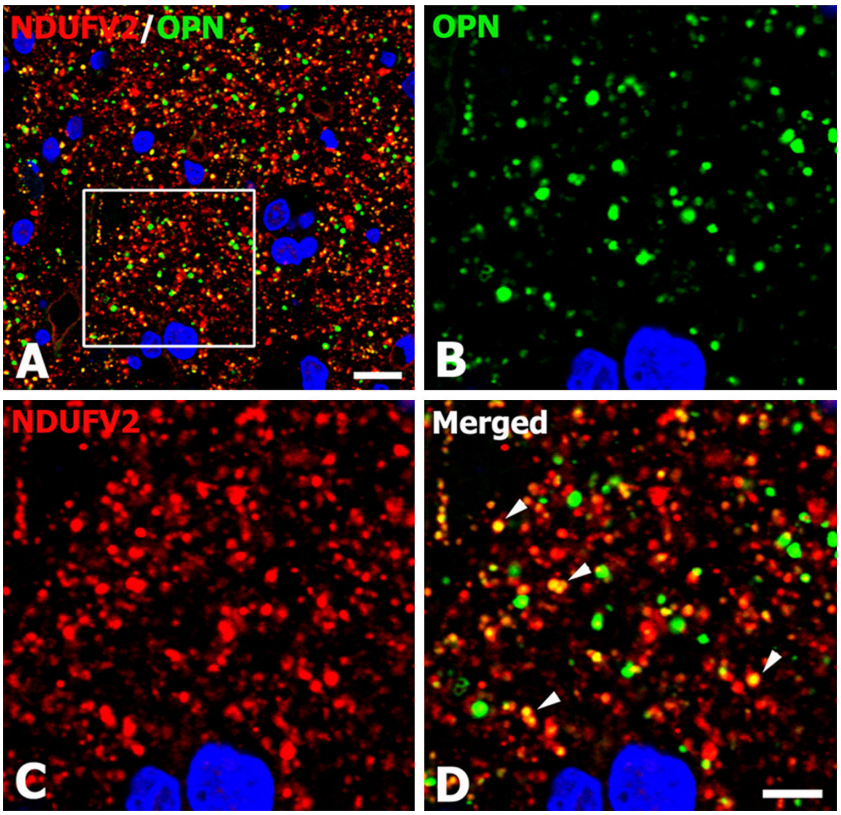

Fig. 3. Relation between osteopontin (OPN) expression and mitochondrial marker demonstrated using confocal microscopy. (**A**) Image showing double immunofluorescence labeling for OPN and mitochondria labeled with NADH dehydrogenase (ubiquinone) flavoprotein 2 (NDUFV2) in the 3NP-injured core. (**B–D**) High magnification of the boxed area in **A**. These images show OPN (**B**) and NDUFV2 (**C**) immunoreactivity, as well as a merged image of both immunolabelings (**D**). Most (but not all) OPN labeling co-localized with NDUFV2 (arrowheads). Bars=10 μm (**A**); 5 μm (**B–D**).

pare Fig. 5D with 5E). These findings indicate that OPN protein is closely associated with degenerating mitochondria in the 3NP-exposed brain.

Neurodegeneration after systemic administration of 3NP selectively occurs in the striatum [4, 7, 32]. It is well known that mitochondria in 3NP-injured neurons present deficits in energy production and failures in calcium buffering because of the inhibition of complex II of the mitochondrial electron transport chain [4, 29, 37, 42], and that MPT leading to the loss of transmembrane potential is caused by uptake and accumulation of calcium in the mitochondria after complex II inhibition [42]. This chain of events causes mitochondrial swelling and the release of cytochrome c, which is an intramitochondrial pro-apoptotic factor [27]. Mitochondria of striatal neurons are particularly vulnerable to MPT induced by a large influx of calcium [10, 32], after which this intracellular calcification then disrupts the structural and functional integrity of the organelles [31, 34]. This is similar to Huntington's disease, in which severe atrophy of the striatum is accompanied by extensive neuronal loss and reactive gliosis [50]. Striatal neuronal loss differs depending on the subpopulation. For example, medium-sized GABAergic spiny neurons are more vulnerable, whereas large cholinergic neurons are less vulnerable in HD [1, 41, 50]. 3NP induced shrunken, dark neurons in the damaged striatum that were positive for GABA immunoreactivity in a series of reports. In addition, several studies suggested that the 'dark' neurons may be associated with phagocytosis, according to OPN expression in various ischemic injuries [13, 17, 18, 25, 43]. In this study, OPN immunoreactivity appearing in the striatal neurons can be classified into two groups. In the first group, OPN protein was expressed in the cell debris of dead neurons or in the mitochondria of degenerating neuron after 3NP induced injury. Based on this, it could be hypothesized that OPN may be expressed in the damaged GABAergic neurons in the striatum, but not in the intact cholinergic neurons. In the second group, OPN was closely associated with calcium precipitation within the mitochondria of degenerating neurons in the 3NP-treated brain. In support of this, Shin *et al.* [44] reported that binding of OPN to the surface of cell fragments is closely associated with calcium precipitation.

In the present study, we observed two different types of OPN immunoreactivity in the mitochondria using immunoelectron microscopy. OPN protein was expressed in the inner membrane and matrix of swelling mitochondria of degenerating neurons, and on the surface of the mitochondria. OPN expression in the degenerated mitochondria was expected to represent calcium precipitates on the mitochondria, although the precise features characteris-

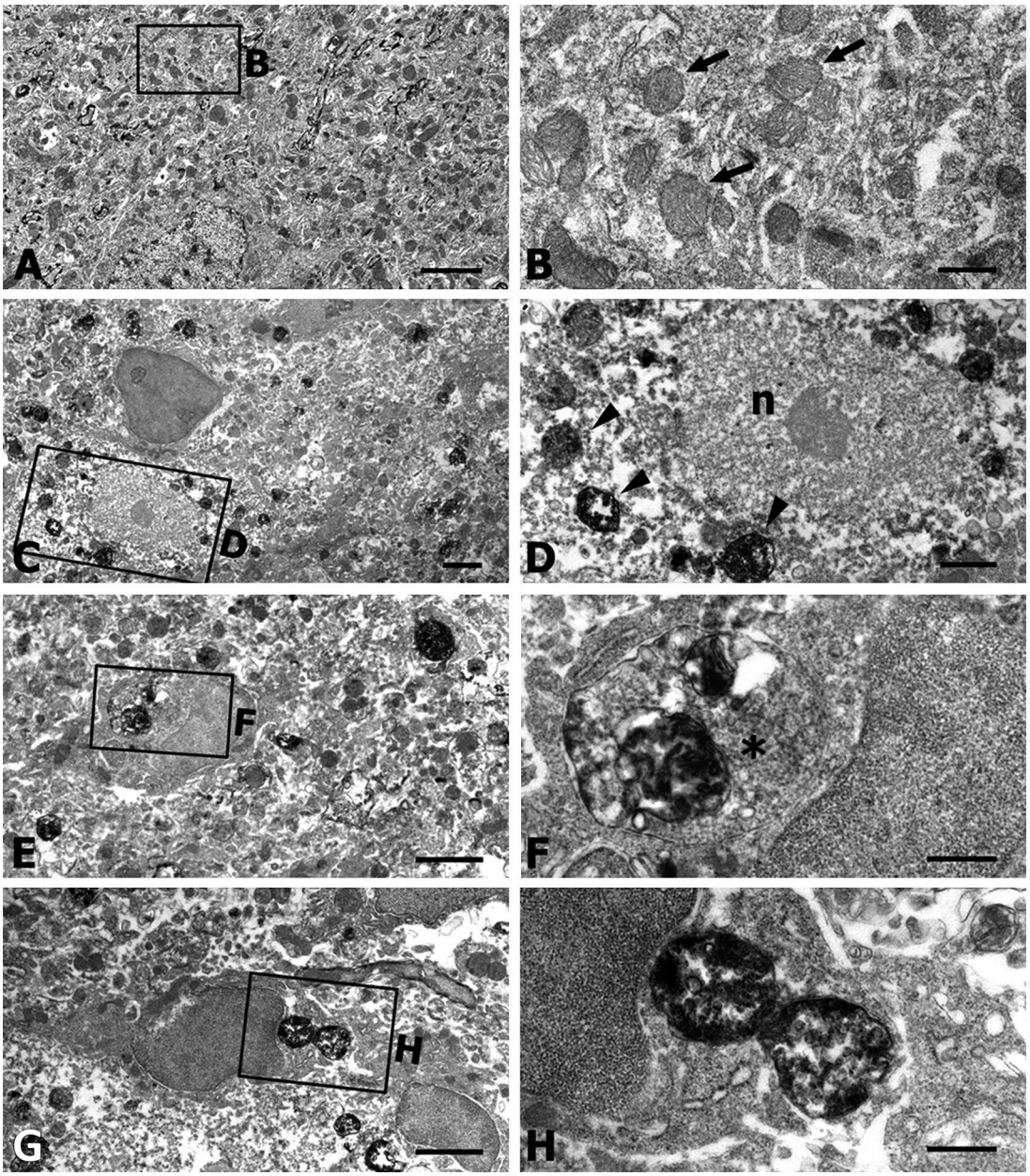

Fig. 4. Electron micrographs showing osteopontin (OPN) labeling using immunoperoxidase immunocytochemistry in the 3-nitropropionic acid (3NP)-injured lesion core. (**A**) OPN expression in the normal striatum is absent. (**B**) Higher magnification of the boxed area in **A** shows normal mitochondria (arrows). (**C**) OPN expression in the 3NP-injured core region appears as strong punctate labeling. (**D**) Higher magnification of the boxed area in **C** shows that OPN is prominently located in the mitochondria (arrowheads) surrounding the nucleus (n) in degenerating neurons. (**E–H**) Microglia are one of the cell types presenting OPN labeling in the 3NP-injured core region. (**F**) Higher magnification of the boxed area in **E**. Note that the microglia demonstrate phagocytic vesicles (asterisk) containing OPN-labeled mitochondria. (**H**) Higher magnification of the boxed area in **G** shows two OPN-labeled mitochondria were engulfed by microglia. Bars=3 μm (**A**); 0.5 μm (**B, F, H**); 2 μm (**C, E, G**); 1 μm (**D**).

tic of this OPN immunolabeling still remain unclear. Our results revealed that OPN expression possibly relates to more diverse changes in the mitochondria than just calcium precipitation. We also tried to detect calcium in the OPN-immunogold labeled mitochondria using electron probe microanalysis (data not shown). A previous study reported that calcium signals were not detected using electron probe microanalysis in a weakly-labeled OPN accumulation site [44]. Tissue preparation for transmission electron microscopy, such as fixation and epon infiltration, alters ionic content and distribution [6, 12, 33]. Therefore, we were unable to detect calcium signals, most likely because the calcium signal was below the threshold for its detection.

Immunoelectron microscopy demonstrated that cell fragments containing OPN-labeled mitochondria were also present within activated brain macrophages. Previous studies showed that OPN is involved in phagocytosis of cell debris in the infarction area after transient focal cerebral

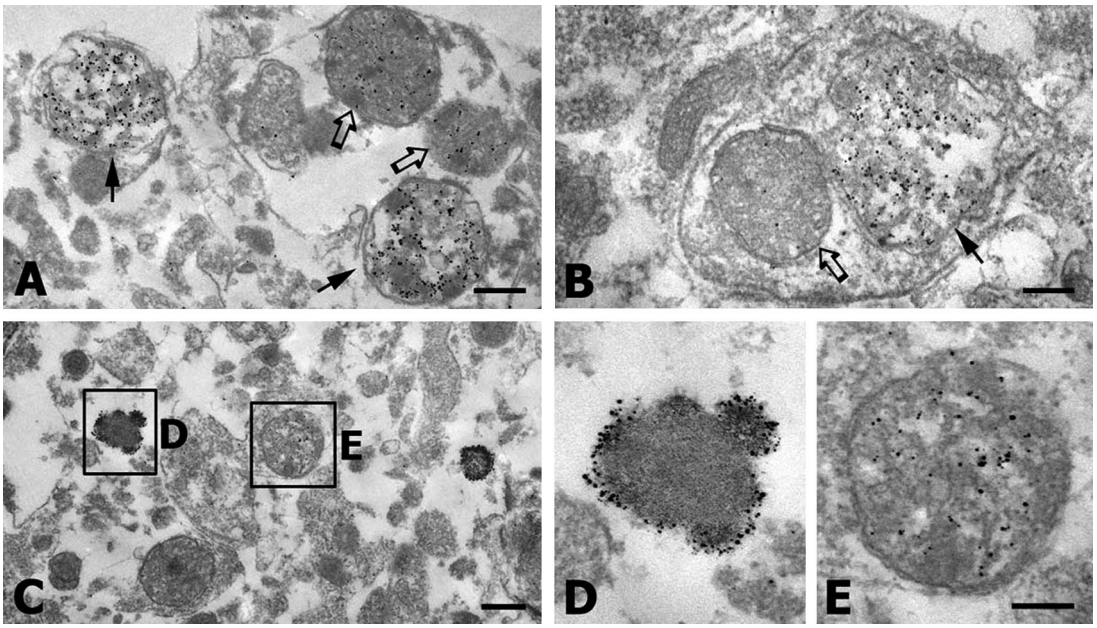

Fig. 5. Electron micrograph showing osteopontin (OPN) labeling using immunogold immunocytochemistry in the 3-nitropropionic acid (3NP)-injured lesion core. (**A, B**) Swelling mitochondria (black arrows) present a larger accumulation of OPN immunogold particles in the inner membrane and the matrix compared to relatively normal-appearing mitochondria (white arrows). (**C–E**) Immunogold particles demonstrate two types of OPN labeling. (**D**) Higher magnification of the boxed area in **C**. OPN immunogold particles are found at the surface of the mitochondria that appear to be small and highly electron-dense. (**E**) Higher magnification of the boxed area in **C**. Immunogold particles are observed in the inner membrane and matrix of swelling mitochondria. Bars=0.4 μm (**A, B**); 0.5 μm (**C**); 0.2 μm (**D, E**).

ischemia [43], and calcium precipitation by binding OPN leads to OPN-mediated phagocytosis by brain macrophages [44]. Strong expression of OPN following ischemic injury contributes to the recruitment of macrophages [51] and OPN has an opsonization function that leads to the facilitation of phagocytosis by macrophages [38]. Thus, our data suggest that OPN protein is closely associated with calcium precipitation within mitochondria in degenerating neurons, and this process is involved in phagocytosis of neuronal debris in 3NP-induced lesions. In addition, taking into account that OPN inhibits mineralization and controls ectopic calcification [45, 47], OPN may have neuroprotective effects on striatal neurons by inhibiting mitochondria dysfunction initiated by mitochondrial calcium overload.

In conclusion, our data showed the spatial relationship between OPN expression and mitochondria in the damaged striatal neurons using confocal and immunoelectron microscopic methods. OPN expression was correlated with the swollen mitochondria of the damaged neurons and brain macrophages after 3NP administration, suggesting that OPN may be involved in the pathogenesis of striatal neuron degeneration, or possibly have neuroprotective effects in 3NP-induced injured striatal neurons by limiting calcium accumulation within the mitochondria.

V. Acknowledgments

This work was supported by the Konkuk University in 2011.

VI. References

1. Albin, R. L., Young, A. B., Penney, J. B., Handelin, B., Balfour, R., Anderson, K. D., Markel, D. S., Tourtellotte, W. W. and Reiner, A. (1990) Abnormalities of striatal projection neurons and N-methyl-D-aspartate receptors in presymptomatic Huntington's disease. *N. Engl. J. Med.* 322; 1293–1298.
2. Alston, T. A., Mela, L. and Bright, H. J. (1977) 3-Nitropropionate, the toxic substance of Indigofera, is a suicide inactivator of succinate dehydrogenase. *Proc. Natl. Acad. Sci. U S A* 74; 3767–3771.
3. Andreyev, A. Y., Fahy, B. and Fiskum, G. (1998) Cytochrome c release from brain mitochondria is independent of the mitochondrial permeability transition. *FEBS Lett.* 439; 373–376.
4. Beal, M. F., Brouillet, E., Jenkins, B. G., Ferrante, R. J., Kowall, N. W., Miller, J. M., Storey, E., Srivastava, R., Rosen, B. R. and Hyman, B. T. (1993) Neurochemical and histologic characterization of striatal excitotoxic lesions produced by the mitochondrial toxin 3-nitropropionic acid. *J. Neurosci.* 13; 4181–4192.
5. Bonnekoh, P., Kuroiwa, T., Kloiber, O. and Hossmann, K. (1992) Time profile of calcium accumulation in hippocampus, striatum and frontoparietal cortex after transient forebrain ischemia in the gerbil. *Acta Neuropathol.* 84; 400–406.
6. Bordat, C., Bouet, O. and Cournot, G. (1998) Calcium distribution in high-pressure frozen bone cells by electron energy loss spectroscopy and electron spectroscopic imaging. *Histochem. Cell Biol.* 109; 167–174.
7. Borlongan, C. V., Koutouzis, T. K. and Sanberg, P. R. (1997) 3-Nitropropionic acid animal model and Huntington's disease. *Neurosci. Biobehav. Rev.* 21; 289–293.
8. Brouillet, E., Guyot, M. C., Mittoux, V., Altairac, S., Conde, F., Palfi, S. and Hantraye, P. (1998) Partial inhibition of brain succinate dehydrogenase by 3-nitropropionic acid is sufficient to initiate striatal degeneration in rat. *J. Neurochem.* 70; 794–805.

9. Brouillet, E., Conde, F., Beal, M. F. and Hantraye, P. (1999) Replicating Huntington's disease phenotype in experimental animals. *Prog. Neurobiol.* 59; 427–468.
10. Brustovetsky, N., Brustovetsky, T., Purl, K. J., Capano, M., Crompton, M. and Dubinsky, J. M. (2003) Increased susceptibility of striatal mitochondria to calcium-induced permeability transition. *J. Neurosci.* 23; 4858–4867.
11. Coles, C. J., Edmondson, D. E. and Singer, T. P. (1979) Inactivation of succinate dehydrogenase by 3-nitropropionate. *J. Biol. Chem.* 254; 5161–5167.
12. Consort Ribeiro, K., Benchimol, M. and Farina, M. (2001) Contribution of cryofixation and freeze-substitution to analytical microscopy: a study of Tritrichomonas foetus hydrogenosomes. *Microsc. Res. Tech.* 53; 87–92.
13. Csordas, A., Mazlo, M. and Gallyas, F. (2003) Recovery versus death of "dark" (compacted) neurons in non-impaired parenchymal environment: light and electron microscopic observations. *Acta Neuropathol.* 106; 37–49.
14. Denhardt, D. T., Noda, M., O'Regan, A. W., Pavlin, D. and Berman, J. S. (2001) Osteopontin as a means to cope with environmental insults: regulation of inflammation, tissue remodeling, and cell survival. *J. Clin. Invest.* 107; 1055–1061.
15. Dux, E., Mies, G., Hossmann, K. A. and Siklos, L. (1987) Calcium in the mitochondria following brief ischemia of gerbil brain. *Neurosci. Lett.* 78; 295–300.
16. Evans, M. C., Griffiths, T. and Meldrum, B. S. (1984) Kainic acid seizures and the reversibility of calcium loading in vulnerable neurons in the hippocampus. *Neuropathol. Appl. Neurobiol.* 10; 285–302.
17. Gallyas, F., Csordas, A., Schwarcz, A. and Mazlo, M. (2005) "Dark" (compacted) neurons may not die through the necrotic pathway. *Exp. Brain Res.* 160; 473–486.
18. Gallyas, F., Kiglics, V., Baracskay, P., Juhasz, G. and Czurko, A. (2008) The mode of death of epilepsy-induced "dark" neurons is neither necrosis nor apoptosis: an electron-microscopic study. *Brain Res.* 1239; 207–215.
19. Gould, D. H. and Gustine, D. L. (1982) Basal ganglia degeneration, myelin alterations, and enzyme inhibition induced in mice by the plant toxin 3-nitropropanoic acid. *Neuropathol. Appl. Neurobiol.* 8; 377–393.
20. Green, D. R. and Reed, J. C. (1998) Mitochondria and apoptosis. *Science* 281; 1309–1312.
21. Gutierrez-Diaz, J. A., Cuevas, P., Reimers, D., Dujovny, M., Diaz, F. G. and Ausman, J. I. (1985) Quantitative electron microscopic study of calcium accumulation in cerebral ischemia mitochondria. *Surg. Neurol.* 24; 67–72.
22. Guyot, M. C., Hantraye, P., Dolan, R., Palfi, S., Maziere, M. and Brouillet, E. (1997) Quantifiable bradykinesia, gait abnormalities and Huntington's disease-like striatal lesions in rats chronically treated with 3-nitropropionic acid. *Neuroscience* 79; 45–56.
23. Karbowski, M. and Neutzner, A. (2012) Neurodegeneration as a consequence of failed mitochondrial maintenance. *Acta Neuropathol.* 123; 157–171.
24. Kodsi, M. H. and Swerdlow, N. R. (1997) Mitochondrial toxin 3-nitropropionic acid produces startle reflex abnormalities and striatal damage in rats that model some features of Huntington's disease. *Neurosci. Lett.* 231; 103–107.
25. Kovesdi, E., Pal, J. and Gallyas, F. (2007) The fate of "dark" neurons produced by transient focal cerebral ischemia in a non-necrotic and non-excitotoxic environment: neurobiological aspects. *Brain Res.* 1147; 272–283.
26. Kowaltowski, A. J. and Vercesi, A. E. (1999) Mitochondrial damage induced by conditions of oxidative stress. *Free Radic. Biol. Med.* 26; 463–471.
27. Liu, X., Kim, C. N., Yang, J., Jemmerson, R. and Wang, X. (1996) Induction of apoptotic program in cell-free extracts: requirement for dATP and cytochrome c. *Cell* 86; 147–157.
28. Ludolph, A. C., He, F., Spencer, P. S., Hammerstad, J. and Sabri, M. (1991) 3-Nitropropionic acid-exogenous animal neurotoxin and possible human striatal toxin. *Can. J. Neurol. Sci.* 18; 492–498.
29. Ludolph, A. C., Seelig, M., Ludolph, A. G., Sabri, M. I. and Spencer, P. S. (1992) ATP deficits and neuronal degeneration induced by 3-nitropropionic acid. *Ann. N. Y. Acad. Sci.* 648; 300–302.
30. Maciel, E. N., Kowaltowski, A. J., Schwalm, F. D., Rodrigues, J. M., Souza, D. O., Vercesi, A. E., Wajner, M. and Castilho, R. F. (2004) Mitochondrial permeability transition in neuronal damage promoted by Ca2+ and respiratory chain complex II inhibition. *J. Neurochem.* 90; 1025–1035.
31. Maetzler, W., Stunitz, H., Bendfeldt, K., Vollenweider, F., Schwaller, B. and Nitsch, C. (2009) Microcalcification after excitotoxicity is enhanced in transgenic mice expressing parvalbumin in all neurones, may commence in neuronal mitochondria and undergoes structural modifications over time. *Neuropathol. Appl. Neurobiol.* 35; 165–177.
32. Mirandola, S. R., Melo, D. R., Saito, A. and Castilho, R. F. (2010) 3-nitropropionic acid-induced mitochondrial permeability transition: comparative study of mitochondria from different tissues and brain regions. *J. Neurosci. Res.* 88; 630–639.
33. Nagata, T. (2004) X-ray microanalysis of biological specimens by high voltage electron microscopy. *Prog. Histochem. Cytochem.* 39; 185–319.
34. Nitsch, C. and Scotti, A. L. (1992) Ibotenic acid-induced calcium deposits in rat substantia nigra. Ultrastructure of their time-dependent formation. *Acta Neuropathol.* 85; 55–70.
35. Ohta, S., Furuta, S., Matsubara, I., Kohno, K., Kumon, Y. and Sakaki, S. (1996) Calcium movement in ischemia-tolerant hippocampal CA1 neurons after transient forebrain ischemia in gerbils. *J. Cereb. Blood Flow Metab.* 16; 915–922.
36. Palfi, S., Ferrante, R. J., Brouillet, E., Beal, M. F., Dolan, R., Guyot, M. C., Peschanski, M. and Hantraye, P. (1996) Chronic 3-nitropropionic acid treatment in baboons replicates the cognitive and motor deficits of Huntington's disease. *J. Neurosci.* 16; 3019–3025.
37. Pang, Z. and Geddes, J. W. (1997) Mechanisms of cell death induced by the mitochondrial toxin 3-nitropropionic acid: acute excitotoxic necrosis and delayed apoptosis. *J. Neurosci.* 17; 3064–3073.
38. Pedraza, C. E., Nikolcheva, L. G., Kaartinen, M. T., Barralet, J. E. and McKee, M. D. (2008) Osteopontin functions as an opsonin and facilitates phagocytosis by macrophages of hydroxyapatite-coated microspheres: implications for bone wound healing. *Bone* 43; 708–716.
39. Puka-Sundvall, M., Gajkowska, B., Cholewinski, M., Blomgren, K., Lazarewicz, J. W. and Hagberg, H. (2000) Subcellular distribution of calcium and ultrastructural changes after cerebral hypoxia-ischemia in immature rats. *Brain Res. Dev. Brain Res.* 125; 31–41.
40. Rangaswami, H., Bulbule, A. and Kundu, G. C. (2006) Osteopontin: role in cell signaling and cancer progression. *Trends Cell Biol.* 16; 79–87.
41. Reiner, A., Albin, R. L., Anderson, K. D., D'Amato, C. J., Penney, J. B. and Young, A. B. (1988) Differential loss of striatal projection neurons in Huntington disease. *Proc. Natl. Acad. Sci. U S A* 85; 5733–5737.
42. Rosenstock, T. R., Carvalho, A. C., Jurkiewicz, A., Frussa-Filho, R. and Smaili, S. S. (2004) Mitochondrial calcium, oxidative stress and apoptosis in a neurodegenerative disease model induced by 3-nitropropionic acid. *J. Neurochem.* 88; 1220–1228.
43. Shin, Y. J., Kim, H. L., Choi, J. S., Choi, J. Y., Cha, J. H. and Lee, M. Y. (2011) Osteopontin: correlation with phagocytosis by

brain macrophages in a rat model of stroke. *Glia* 59; 413–423.
44. Shin, Y. J., Kim, H. L., Park, J. M., Cho, J. M., Kim, C. Y., Choi, K. J., Kweon, H. S., Cha, J. H. and Lee, M. Y. (2012) Overlapping distribution of osteopontin and calcium in the ischemic core of rat brain after transient focal ischemia. *J. Neurotrauma*. 29; 1530–1538.
45. Shiraga, H., Min, W., VanDusen, W. J., Clayman, M. D., Miner, D., Terrell, C. H., Sherbotie, J. R., Foreman, J. W., Przysiecki, C., Neilson, E. G. and Hoyer, J. R. (1992) Inhibition of calcium oxalate crystal growth in vitro by uropontin: another member of the aspartic acid-rich protein superfamily. *Proc. Natl. Acad. Sci. U S A* 89; 426–430.
46. Shirotani, T., Shima, K., Iwata, M., Kita, H. and Chigasaki, H. (1994) Calcium accumulation following middle cerebral artery occlusion in stroke-prone spontaneously hypertensive rats. *J. Cereb. Blood Flow Metab.* 14; 831–836.
47. Steitz, S. A., Speer, M. Y., McKee, M. D., Liaw, L., Almeida, M., Yang, H. and Giachelli, C. M. (2002) Osteopontin inhibits mineral deposition and promotes regression of ectopic calcification. *Am. J. Pathol.* 161; 2035–2046.
48. Sztriha, L., Joo, F. and Szerdahelyi, P. (1985) Accumulation of calcium in the rat hippocampus during kainic acid seizures. *Brain Res.* 360; 51–57.
49. Vis, J. C., Verbeek, M. M., De Waal, R. M., Ten Donkelaar, H. J. and Kremer, H. P. (1999) 3-Nitropropionic acid induces a spectrum of Huntington's disease-like neuropathology in rat striatum. *Neuropathol. Appl. Neurobiol.* 25; 513–521.
50. Vonsattel, J. P. and DiFiglia, M. (1998) Huntington disease. *J. Neuropathol. Exp. Neurol.* 57; 369–384.
51. Wang, K. X. and Denhardt, D. T. (2008) Osteopontin: role in immune regulation and stress responses. *Cytokine Growth Factor Rev.* 19; 333–345.
52. Watanabe, H., Kumon, Y., Ohta, S., Sakaki, S., Matsuda, S. and Sakanaka, M. (1998) Changes in protein synthesis and calcium homeostasis in the thalamus of spontaneously hypertensive rats with focal cerebral ischemia. *J. Cereb. Blood Flow Metab.* 18; 686–696.
53. Wullner, U., Young, A. B., Penney, J. B. and Beal, M. F. (1994) 3-Nitropropionic acid toxicity in the striatum. *J. Neurochem.* 63; 1772–1781.
54. Zamzami, N., Marchetti, P., Castedo, M., Decaudin, D., Macho, A., Hirsch, T., Susin, S. A., Petit, P. X., Mignotte, B. and Kroemer, G. (1995) Sequential reduction of mitochondrial transmembrane potential and generation of reactive oxygen species in early programmed cell death. *J. Exp. Med.* 182; 367–377.